Available online at www.sciencedirect.com
ScienceDirect
Journal of Molecular Catalysis A: Chemical 281 (2008) 214–218
JOURNAL OF MOLECULAR CATALYSIS A: CHEMICAL
www.elsevier.com/locate/molcata

Solid-state NMR strategies for characterizing high surface area niobates

Xuefeng Wang, Luis J. Smith *

Clark University, Department of Chemistry, 950 Main Street, Worcester, MA 01610, USA

Available online 22 November 2007

Abstract

Layered niobates have been found to be strong solid-acid catalysts and have high surface areas while maintaining their crystalline structure. These materials can serve as model compounds for the metal environments at the surface of amorphous solid-acid niobates. The niobium environment in $KCa_2Nb_3O_{10}$ and its acid exchanged version were studied using ^{93}Nb solid-state NMR. As ^{93}Nb is a quadrupolar nucleus, both the electric field gradient (EFG) and chemical shift anisotropy (CSA) for a given site can yield information about the symmetry of the local structure and relate its influence on the acid site. The change in the local environment of surface niobium sites upon acid exchange is observed via NMR and attributed to changes in the terminal niobium–oxygen bonds.

Keywords: Nuclear magnetic resonance; Niobium oxide; Solid acid

1. Introduction

The local structure at the surface of oxides can change in response to species present at the surface. These perturbations in structure can affect the acidity of the oxygen atoms at the surface [1,2] and potentially affect the reactivity of the material. Recent developments in solid-state NMR methodology to study quadrupolar nuclei permit the examination of elements in highly anisotropic environments at the oxide surface and the discrimination of different types of environments that may be present at the surface. Following this approach, the local structures of niobium atoms in a layered niobate have been determined and a change in local structure at the interface has been observed when the cations in the interlayer gallery are altered. The methods applied to examine the ^{93}Nb nucleus are applicable to other quadrupolar nuclei and are not dependent on long-range order being present in the material. With this strategy, the structure and structural changes at the surface of metal oxides can be studied in detail and add to the understanding of how the material surface plays a role in its properties.

Layered transitional metal oxides have garnered some interest as potential solid-acid catalysts [3–5]. Acid exchange of alkali cation forms of these layered oxides can produce potentially strong acids but are limited due to the small interlayer distances. Exfoliation via soft chemical methods has been pursued as a strategy to increase the available surface area of the materials. While the overall structure of the layers is maintained through these soft chemical procedures, small variations in the structure of the surface are possible.

One such layered niobate is $KCa_2Nb_3O_{10}$, which can be easily acid exchanged [6]. $KCa_2Nb_3O_{10}$ is a member of the Dion-Jacobson family of layered perovskites. The structure consists of triple perovskite layers separated by a single layer of potassium cations [7]. The perovskite layer consists of niobia octahedra that share vertices and calcium cations nested between the connected polyhedra in 12-coordinate sites (Fig. 1). In this structure, there are two distinct octahedral sites for the niobium cations, one site, designated Nb(1), in the interior of the layers and one at the interface of the layers, designated Nb(2). A 1:2 ratio exists between the population of sites in the center of the layers and sites at the interface. The niobium cations in the interface site sit in distorted environments with terminal Nb–O bonds that have a length of 1.75 Å for the bonds that point away from the layer and 2.39 Å for the bonds that point toward the layer. The remaining four bonds have lengths in the range of 1.97–2.02 Å. As a result the niobium site at the interface could almost be considered five-coordinate if the long Nb–O bond is ignored. The site in the center of the layer is more isotropic than the interface site. Six Nb–O bonds that range in

* Corresponding author. Tel.: +1 508 793 7753; fax: +1 508 793 8861.
E-mail addresses: xwang@clarku.edu (X. Wang), lusmith@clarku.edu (L.J. Smith).

1381-1169/$ – see front matter © 2007 Elsevier B.V. All rights reserved.
doi:10.1016/j.molcata.2007.11.015

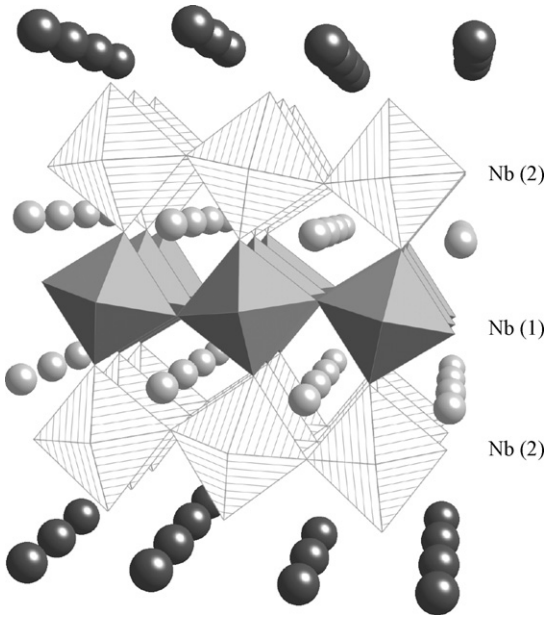

Fig. 1. $KCa_2Nb_3O_{10}$ structure with the NbO_6 octahedra shown as filled polyhedra and the two niobium sites designated by dark (Nb(1)) and light (Nb(2)) shades. The calcium cations are shown as light spheres and the potassium cations as dark spheres.

length from 1.91 to 2.02 Å surround the niobium cation at this site.

NMR can describe the nature of the niobium environment in this oxide. The niobium nucleus is perturbed by magnetic interactions with surrounding bonding electrons and adjacent nuclei and by electric interactions with the gradient created by local charges. The resulting ^{93}Nb solid-state spectrum can be substantially broadened as all possible angular orientations in a powdered sample are observed. Broad static solid-state spectra have reduced resolution and identification of different environments in the sample becomes difficult due to substantial overlap of the spectral patterns. Sample spinning at a fixed angle with reference to the magnetic field, the "magic angle", reduces the broadening of observed NMR transitions in solidified systems such that high-resolution experiments are possible. Interactions with the bonding electrons and variations in the local bond environment are manifested through the chemical shift anisotropy (CSA) and magic angle spinning averages this interaction to an isotropic chemical shift. Non-spinning experiments permit the measurement of the tensor that describes the CSA, which can be described in terms of a span (largest width of the CSA powder pattern) and a skew (describing the symmetry of the tensor) [8]. As the components of the CSA depend primarily on the local bonding environment, the interaction effectively probes the influence of the nearest neighbors only.

Interactions with the electric field gradient (EFG) surrounding an atom due to the distribution of charges in the material perturb the observed solid-state NMR spectrum only if the nuclei are quadrupolar (having a nuclear spin number greater than one-half), which is the case for approximately 75% of the periodic table. ^{93}Nb is a quadrupolar nucleus with a spin number of 9/2 and a natural abundance of 100%. The magnitude and symmetry of the EFG surrounding the observed atom in the NMR experiment will determine the size of the perturbation. Measurement of the magnitude of the anisotropy of the EFG, known as the quadrupolar coupling (C_Q), can give explicit information about the local environment since it measures the largest component (V_{ZZ}) of the EFG tensor. The symmetry of the tensor can be determined from the asymmetry parameter calculated from the tensor components $((V_{XX} - V_{YY})/V_{ZZ})$ when the tensor components are defined as $|V_{ZZ}| \geq |V_{YY}| \geq |V_{XX}|$ [9], as will be the case in this paper.

When the quadrupolar coupling is large enough that the broadening of the spectrum is much larger in frequency than the spinning rate, MAS is no longer sufficient to reduce the broadening. This is often the case with niobium based oxides [10–13]. Line narrowing of resonances with extremely large quadrupolar coupling values can be achieved via the Quadrupolar Phase Adjusted Sideband Suppression (QPASS) method which yields an "infinite" spinning rate line shape from data collected at conventional spinning rates [14]. The result is a simplified pattern yielding a line shape only dependent on the quadrupolar interaction from which EFG information can be extracted. One difficulty with the QPASS method is that the resulting signals have low intensity with long data acquisition times of up to several days. Signal enhancement methods for quadrupolar nuclei such as Rotor Assisted Population Transfer (RAPT) [15–17] can substantially decrease the data acquisition time and can selectively enhance signals based on the magnitude of the quadrupolar coupling allowing for the selective examination of metal sites based on their local symmetry. An experiment to remove the signal of small EFG sites while retaining large EFG site information in the final QPASS spectrum, the $\pi/2$-RAPT-QPASS pulse sequence, has been developed [18].

The correlation between pairs of different elements in a sample based on their relative proximity is possible with solid-state NMR through the dipolar interaction between the nuclear magnetic moments of a pair of atoms. Cross polarization (CP) can transfer signal polarization from hydrogen nuclei to an adjacent atom within a distance of 0.1–1 nanometers [19]. Distance based correlations can be obtained through the transfer of signal polarization between adjacent atoms using this method. Typically, CP is coupled with MAS to improve the resolution of the resulting signal. However, for quadrupolar nuclei CPMAS is often ineffective with little or no polarization transfer occurring for systems with large quadrupolar coupling values [20]. Non-spinning CP experiments can still yield structural information despite the low resolution due to the broad spectrum [21].

In this paper, we demonstrate approaches for determining the structural information for quadrupolar nuclei, such as ^{93}Nb, in oxide materials. Through a combination of MAS based methods, such as QPASS and RAPT, and non-spinning experiments, such as CP, the local structure NMR information for the two niobium sites in $KCa_2Nb_3O_{10}$ and its acid exchanged form were determined. A modification in the structure of the niobium site at the interface of the layers in the oxide upon ion exchange

was observed and is explained as a result of changes in the bond length of the Nb–O terminal bond.

2. Experimental

The $KCa_2Nb_3O_{10}$ was prepared via microwave synthesis. A mixture of K_2SO_4, $CaSO_4$, and Nb_2O_5 was pressed into a pellet with the mole ratio of 10:2:3 for K:Ca:Nb. The pellet was heated in a bed of activated charcoal (Darco-G60) in a porcelain crucible, which in turn was placed in a sand bed to absorb the emitted heat from the crucible. The materials were irradiated in a 1200 W domestic microwave oven for 5–10 min at 90% power to produce the desired phase. The samples were then washed with distilled water and allowed to dry at room temperature. To produce the acid form, $KCa_2Nb_3O_{10}$ was treated with 6 M HNO_3 for 1 week at 80 °C [22]. After acid treatment, the product was filtered and washed with distilled water and dried at 110 °C. Phase identity was determined using X-ray powder diffraction on a Bruker AXS D8 Focus diffractometer and the reflections were compared to the literature [6,7].

All NMR data were collected using 200 MHz Mercury and 400 MHz Unity Inova spectrometers with ^{93}Nb resonance frequencies of 48.94 and 97.74 MHz, respectively. Variable offset cumulative spectra (VOCS) [23] echo data were constructed from 7 Hahn echo spectra collected with an offset difference of 78.125 kHz and with a radio frequency field strength of 20 kHz. MAS and QPASS data were collected on the 400 MHz Unity INOVA spectrometer using a Chemagnetics 2.5 mm double-resonance MAS probe with a spinning rate of 20 kHz. Selective pulses used in all experiments had a radio frequency field strength of 20 kHz yielding selective $\pi/2$ and π pulses of 2.5 and 5.0 μs, respectively. For both the non-selective QPASS and the $\pi/2$-RAPT-QPASS sequences, a multiple-rotor cycle version of QPASS [24] was used and utilized 8 sets of timings. RAPT enhancements used a variable offset Gaussian pulse train with a radio frequency strength of 83 kHz and a Gaussian pulse shape consisting of a pulse length of 12 μs with a σ of 2.975 μs, such that the full width at half maximum of the pulse shape is 2.35σ. Frequency offsets of 700 kHz and 1.6 MHz were used for the non-selective and selective RAPT-based experiments. The non-spinning CP experiments were collected using the 400 MHz Unity INOVA spectrometer with a ^{1}H resonance frequency of 399.76 MHz and used the VOCS method to construct the final spectrum with an offset difference of 39.0625 kHz and utilized radio frequency strengths of 13 kHz for ^{93}Nb and 65 kHz for ^{1}H with a contact time of 2 ms.

All spectra are referenced to $NbCl_5$ in acetonitrile (0 ppm). All data were processed using the RMN processing program [25] for the Macintosh. The QPASS data were fit using DMFIT2006 [26] with the errors for the parameters calculated by the software. Simulations of the static patterns were achieved through iterative fitting using WSOLIDS [27]. Errors for the NMR parameters determined using the WSOLIDS programs were estimated based both on visual inspection and on the change in the parameter that yielded a doubling in the sum of the squares of the deviation of the observed data from the model.

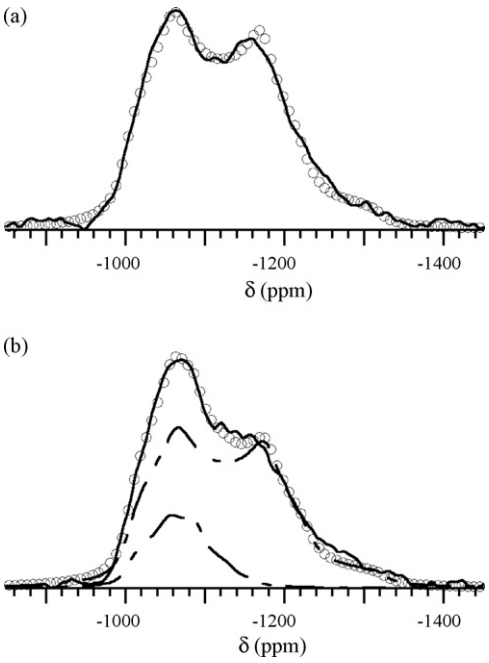

Fig. 2. (a) ^{93}Nb $\pi/2$-RAPT-QPASS spectrum and fit of $KCa_2Nb_3O_{10}$ and (b) ^{93}Nb QPASS spectrum and fit (solid line: data, open circles: fit, dashed line: individual site line shapes).

3. Results and discussion

^{93}Nb QPASS experiments coupled with the RAPT excitation were collected on $KCa_2Nb_3O_{10}$ to determine the information on the isotropic chemical shift and the EFG information for the two niobium sites in the material. The $\pi/2$-RAPT-QPASS experiment yielded information on the more anisotropic site with a C_Q value of 31.2 ± 0.6 MHz, an asymmetry parameter of 0.30 ± 0.02 and an isotropic chemical shift of -976 ± 5 ppm (Fig. 2a). With the information on the large C_Q site, the spectra from non-selective RAPT-QPASS experiment (Fig. 2b) was analyzed to yield information on the smaller C_Q niobium site in the material. The more isotropic site had a C_Q value of 21.5 ± 0.5 MHz, an asymmetry parameter of 0.75 ± 0.05, and an isotropic chemical shift of -998 ± 3 ppm. Using the intensity ratio of 20:80 for isotropic to anisotropic site, the more anisotropic site was assigned to the niobium atom located at the interface between the layers, Nb(2), while the less anisotropic site was assigned to the niobium located in the interior of the layer, Nb(1) [18]. The population ratios follow the observed trend based on the crystal structure but does not match the ratio. Since a non-selective RAPT-QPASS experiment was used to compare the intensities of the two sites, the ratio of intensities must be used with caution. The RAPT enhancement will be affected by the magnitude of the C_Q values for the two sites. The choice of frequency offset in the RAPT based experiment is dependent on the C_Q values and affects the maximum possible enhancement for a particular site. Due to the large difference in C_Q values for the two sites, no frequency offset could result in similar enhancements for the sites.

Examination of the $KCa_2Nb_3O_{10}$ sample under static conditions permits the determination of the CSA parameters for a

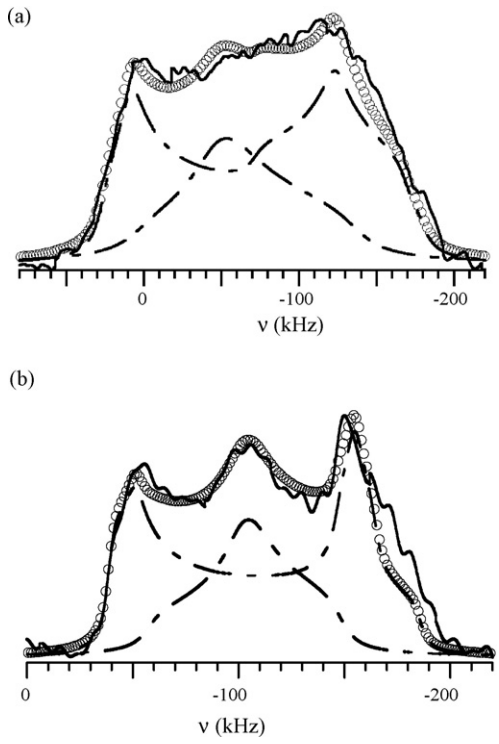

Fig. 3. ^{93}Nb VOCS static spectrum and fit of $KCa_2Nb_3O_{10}$ (a) at 48.94 MHz and (b) at 97.74 MHz (solid line: data, open circles: fit, dashed line: individual site line shapes).

complete description of the niobium environment. Non-spinning ^{93}Nb spectra were collected and combined following the VOCS method to produce a single broad spectrum (Fig. 3a and b). Fitting of the spectrum was possible using the EFG information derived from the QPASS experiments. The fit yielded for the interface site, Nb(2), a span of 910 ± 80 ppm and a skew of 0.6 ± 0.2 to describe the CSA tensor with the Euler angles describing the relative orientation of the EFG and CSA tensors as $\alpha = 75 \pm 15^\circ$, $\beta = 0 \pm 9^\circ$ and $\gamma = 50 \pm 25^\circ$. The CSA tensor values for the isotropic site, Nb(1), were determined to be a span of 380 ± 40 ppm and a skew of -0.7 ± 0.2 with Euler angles of $\alpha = 5 \pm 20^\circ$, $\beta = 0 \pm 25^\circ$ and $\gamma = 5 \pm 30^\circ$. As was observed with the QPASS data, the niobium site at the interface appears to have a substantially larger anisotropic interaction than the interior site despite the fact that the interior niobium is adjacent to the interface. The large anisotropy of the interface is expected, as one of the oxygen atoms is coordinated to only one niobium with a short bond length. Such vast differences in the EFG and CSA values can be utilized to discriminate between the interface region of the material and the niobium sites removed from that interface.

Using the EFG and CSA information derived for the $KCa_2Nb_3O_{10}$ sample, the static ^{93}Nb VOCS final spectrum was collected and fit for the acid exchanged version (Fig. 4a and b). From the width of the signal it is clear that a decrease in some of the anisotropies has occurred upon the exchange of K^+ with H^+. The isotropic chemical shift of the interface and interior sites were found to have changed to -1180 ± 20 and -1160 ± 35 ppm, respectively. The EFG for the interior site

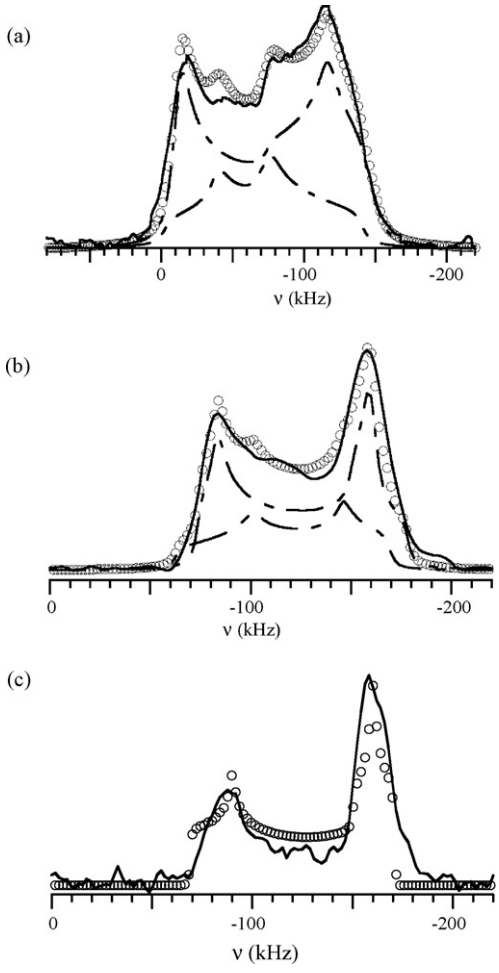

Fig. 4. ^{93}Nb VOCS static spectrum and fit of acid exchanged $KCa_2Nb_3O_{10}$ (a) at 48.94 MHz and (b) at 97.74 MHz (solid line: data, open circles: fit, dashed line: individual site line shapes), (c) ^{93}Nb static CP spectrum of acid exchanged $KCa_2Nb_3O_{10}$ (solid line) and powder pattern simulation using surface niobium site parameters (open circles).

was essentially the same as in the K^+ version with a C_Q of 21.5 ± 1.0 MHz and an asymmetry parameter of 0.75 ± 0.15. The CSA for the interior site did change with a span of 720 ± 80 ppm and a skew of 0.0 ± 0.3 with Euler angles of $\alpha = 12 \pm 35^\circ$, $\beta = 7 \pm 30^\circ$ and $\gamma = 25 \pm 45^\circ$ for the relative orientation of the two tensors. For the interface site, a decrease in the size of the EFG anisotropy was observed with a new C_Q value of 26.9 ± 1.3 MHz while the asymmetry parameter changed only slightly to 0.3 ± 0.1. The CSA decreased as well with values for the span and skew of 640 ± 60 ppm and 0.5 ± 0.2, respectively, with Euler angles of $\alpha = 85 \pm 15^\circ$, $\beta = 5 \pm 10^\circ$ and $\gamma = 20 \pm 20^\circ$.

A CP experiment was conducted on a static sample to transfer polarization from the hydrogen to neighboring niobium atoms. The resulting spectrum (Fig. 4c) differed from the VOCS spectrum for the acid form. Intensity was lost from the center of the spectrum. However, the CP spectrum could be fit solely with the EFG and CSA parameters for the interfacial niobium site. The loss in intensity in the center corresponds to the loss of the signal from the interior site. The CP experiment allowed only the interface site to be viewed and further confirmed the assignment of the large EFG to the surface site.

The results of the CP experiment show that the local structure of the interface site, Nb(2), has changed in response to protonation. The change in the EFG and CSA was limited primarily to the size of the anisotropies, C_Q and span, while the symmetries of the tensors remained essentially unchanged. The decrease in the sizes of the EFG and CSA for the Nb(2) site points to a reduction in the distortion of the niobium octahedra at the interface. Protonation of the terminal oxygen, which points toward the interlayer gallery, would cause the bond between niobium and this oxygen atom to weaken and lengthen as electron density from the oxygen atom is donated to the hydrogen atom present at the surface. The redistribution of the electron density surrounding the niobium nucleus most likely also alters the bond to the bridging oxygen shared with the interior octahedra. The bond would be shorter and would result in the niobium atom shifting closer to the center of the octahedron. The change in bond lengths along the direction of the short and long Nb–O bonds would not change the square pyramidal symmetry of the site much but could reduce the EFG and CSA.

The change in the bonding in the interface site, Nb(2), would in turn alter the bonding of the interior site, Nb(1). The strengthening of the Nb–O bond between Nb(2) and the oxygen atom shared with Nb(1) would in turn weaken the bond between Nb(1) and this bridging oxygen atom. This change in bonding for the interior site would distort the local symmetry. This distortion may account for the observed increase in the CSA for the Nb(1) site. Without additional information, only qualitative arguments can be made to link the NMR parameters to the changes in the crystallographic structure. Further elaboration of the relationship between the change in the EFG and the change in bond length is possible through ab initio quantum calculations [28], which are currently being pursued.

4. Conclusion

Using ^{93}Nb NMR, the sites in a layered niobate, $KCa_2Nb_3O_{10}$, were characterized in terms of the EFG and chemical shift anisotropy. Ion exchange from the potassium form to an acidic form resulted in a change in the local environments of the two niobium sites. Using cross polarization techniques, the information for the niobium environment at the surface was isolated and the reduction in the distortion of the interfacial niobium site was more clearly observed. The decrease of the EFG and chemical shift anisotropy points to an increase in the bond length of the terminal Nb–O bond at the surface and a relaxation in the distortion of the NbO_6 octahedron in response to the protonation of the surface.

Acknowledgement

The X-ray powder diffraction equipment was supported by the Kresge Foundation Science Initiative.

References

[1] N.S.P. Bhuvanesh, J. Gopalakrishnan, J. Mater. Chem. 7 (1997) 2297–2306.
[2] T. Hiemstra, P. Venema, W.H. VanRiemsdijk, J. Colloid Interface Sci. 184 (1996) 680–692.
[3] A. Takagaki, M. Sugisawa, D.L. Lu, J.N. Kondo, M. Hara, K. Domen, S. Hayashi, J. Am. Chem. Soc. 125 (2003) 5479–5485.
[4] A. Takagaki, T. Yoshida, D.L. Lu, J.N. Kondo, M. Hara, K. Domen, S. Hayashi, J. Phys. Chem. B 108 (2004) 11549–11555.
[5] A. Takagaki, D.L. Lu, J.N. Kondo, M. Hara, S. Hayashi, K. Domen, Chem. Mater. 17 (2005) 2487–2489.
[6] A.J. Jacobson, J.T. Lewandowski, J.W. Johnson, J. Less-Common Metals 116 (1986) 137–146.
[7] H. Fukuoka, T. Isami, S. Yamanaka, J. Solid State Chem. 151 (2000) 40–45.
[8] J. Herzfeld, A.E. Berger, J. Chem. Phys. 73 (1980) 6021–6030.
[9] S.E. Ashbrook, M.J. Duer, Concepts Magn. Reson. Part A 28A (2006) 183–248.
[10] S. Prasad, P. Zhao, J. Huang, J.J. Fitzgerald, J.S. Shore, Solid State Nucl. Magn. Reson. 19 (2001) 45–62.
[11] G.L. Hoatson, D.H.H. Zhou, F. Fayon, D. Massiot, R.L. Vold, Phys. Rev. B 66 (2002) 224103.
[12] L.S. Du, R.W. Schurko, N. Kim, C.P. Grey, J. Phys. Chem. A 106 (2002) 7876–7886.
[13] O.B. Lapina, D.F. Khabibulin, K.V. Romanenko, Z.H. Gan, M.G. Zuev, V.N. Krasil'nikov, V.E. Fedorov, Solid State Nucl. Magn. Reson. 28 (2005) 204–224.
[14] D. Massiot, V. Montouillout, F. Fayon, P. Florian, C. Bessada, Chem. Phys. Lett. 272 (1997) 295–300.
[15] Z. Yao, H.T. Kwak, D. Sakellariou, L. Emsley, P.J. Grandinetti, Chem. Phys. Lett. 327 (2000) 85–90.
[16] H.T. Kwak, S. Prasad, T. Clark, P.J. Grandinetti, J. Magn. Reson. 160 (2003) 107–113.
[17] H.T. Kwak, S. Prasad, T. Clark, P.J. Grandinetti, Solid State Nucl. Magn. Reson. 24 (2003) 71–77.
[18] L.J. Smith, C. Seith, J. Magn. Reson. 179 (2006) 164–168.
[19] A. Pines, M.G. Gibby, J.S. Waugh, J. Chem. Phys. 59 (1973) 569–590.
[20] J.P. Amoureux, M. Pruski, Mol. Phys. 100 (2002) 1595–1613.
[21] A.S. Lipton, J.A. Sears, P.D. Ellis, J. Magn. Reson. 151 (2001) 48–59.
[22] S. Hardin, D. Hay, M. Millikan, J.V. Sanders, T.W. Turney, Chem. Mater. 3 (1991) 977–983.
[23] D. Massiot, I. Farnan, N. Gautier, D. Trumeau, A. Trokiner, J.P. Coutures, Solid State Nucl. Magn. Reson. 4 (1995) 241–248.
[24] D.J. Aurentz, F.G. Vogt, K.T. Mueller, A.J. Benesi, J. Magn. Reson. 138 (1999) 320–325.
[25] P.J. Grandinetti, RMN, Version 1.3.0, Department of Chemistry, Ohio State University, Columbus, OH, 2005.
[26] D. Massiot, F. Fayon, M. Capron, I. King, S. Le Calve, B. Alonso, J.O. Durand, B. Bujoli, Z.H. Gan, G. Hoatson, Magn. Reson. Chem. 40 (2002) 70–76.
[27] K. Eichele, R.E. Wasylishen, WSOLIDS, Version 1.17.30, University of Tuebingen, Tuebingen, Germany, 2001.
[28] J.B.D. de Lacaillerie, F. Barberon, K.V. Romanenko, O.B. Lapina, L. Le Polles, R. Gautier, Z.H. Gan, J. Phys. Chem. B 109 (2005) 14033–14042.